

STRUCTURAL AND ELECTRONIC PROPERTIES OF CHALCOPYRITE SEMICONDUCTORS

By

Bijayalaxmi Panda

Under the Guidance of
Prof. Biplab Ganguli



Department Of Physics

National Institute Of Technology, Rourkela

CERTIFICATE

This is to certify that the project thesis entitled ” Structural and electronic properties of chalcopyrite semiconductor” being submitted by Bijay-alaxmi Panda in partial fulfilment to the requirement of the one year project course (PH 592) of MSc Degree in physics of National Institute of Technology, Rourkela has been carried out under my supervision. The result incorporated in the thesis has been produced by using TB-LMTO codes.

Prof. Biplab Ganguli
Dept. of Physics
National Institute of
Technology
Rourkela - 769008

ACKNOWLEDGEMENT

I would like to acknowledge my guide Prof. Biplab Ganguli for his help and guidance in the completion of my one-year project and also for his enormous motivation and encouragement. I am also very much thankful to Phd scholars of computational physics lab whose encouragement and support helped me to complete my project.

ABSTRACT

We have studied the structural and electronic properties of pure, defect and doped chalcopyrite semiconductors using Density functional theory (DFT) based first principle technique within Tight binding Linear Muffin Tin orbital (TB-LMTO) method. Our calculated structural parameters such as lattice constant, anion displacement parameter(u) in case of pure chalcopyrite and anion displacement parameter(u_x, u_y, u_z) in case of defect and doped chalcopyrite, tetragonal distortion($\eta=c/2a$) and bond length are in good agreement with other work. Our band structure calculation suggest that most of chalcopyrites are direct band gap semiconductors. In our study the $CuInSe_2$ is a direct bandgap semiconductor having band gap = 1.35 eV. Calculated band gaps are in good agreement with other experimental and theoretical works with LDA limitation.

Contents

1	INTRODUCTION	6
2	MATERIAL PROPERTIES OF CHALCO- PYRITE	8
2.0.1	METHODOLOGY	8
2.1	CRYSTAL STRUCTURE OF CHALCO-	8
2.1.1	ZINC BLEND STRUCTURE	10
2.1.2	STRUCTURE OF CHALCOPYRITE	10
3	TYPES OF CHALCOPYRITES	12
4	PURE CHALCOPYRITE AND ITS STRUCTURAL AND ELECTRONIC -PROPERTIES	12
4.1	STRUCTURAL PROPERTIES OF PURE CHA- LCOPYRITE	13
4.1.1	STRUCTURE OF PURE CHALCOPYRITE . .	14
4.2	ELECTRONIC PROPERTIES OF PURE CHAL- COPYRITE	16
4.2.1	METHODOLOGY :	16
4.2.2	RESULT AND DISCUSSION	16
5	DEFFECT CHALCOPYRITE AND ITS STRUCTURAL AND ELECTRONIC -PROPERTIES	18
5.1	STRUCTURAL PROPERTIES OF DEFECT CH- ALCOPYRITE	19
5.1.1	CRYSTAL STRUCTURE OF DEFECT CHALC- . . .	20
5.2	ELECTRONIC PROPERTIES OF DEFECT CHA- LCOPYRITE	21
5.2.1	METHODOLOGY :	21
5.2.2	RESULT AND DISCUSSION	21
6	DOPED CHALCOPYRITE AND ITS STRUCTURAL AND ELECTRONIC -PROPERTIES	24
6.1	STRUCTURAL PROPERTIES OF DOPED CHA- . .	25

6.1.1	CRYSTAL STRUCTURE OF DOPED CHALCO- PYRITE :	25
6.2	ELECTRONIC PROPERTIES OF DOPED CHAL-	25
6.2.1	METHODOLOGY	26
6.2.2	RESULT AND DISCUSSION	26
7	APPLICATION OF CHALCOPYRITE	29
8	CONCLUSION	30
9	REFERENCES	31

1 INTRODUCTION

There is a strong demand for renewable energies due to the limited availability of fossil and nuclear fuels and due to growing environmental problems. Currently, the cost for photovoltaic systems is one of the main obstacles preventing production and application on a large scale.

Ternary chalcopyrites with the general formula $A^I B^{III} C_2$ ($A = \text{Li, Na, Cu, Ag}$; $B = \text{Al, Ga, In}$; $C = \text{S, Se, Te}$) are of considerable interest because of their potential optoelectronic applications as solar energy converters, nonlinear optical (NLO) devices, light emitting diodes (LED), and detectors. Polycrystalline solar cells with a Cu(In, Ga)Se_2 absorber reached recently up to 18.8 % . Chalcopyrite is a type of semiconductor .

Ternary chalcopyrites with the general formula $A^I B^{III} C_2$ ($A = \text{Li, Na, Cu, Ag}$; $B = \text{Al, Ga, In}$; $C = \text{S, Se, Te}$) are of considerable interest because of their potential optoelectronic applications as solar energy converters, nonlinear optical (NLO) devices, light emitting diodes (LED), and detectors . Usually, these compounds belong to two crystallographic categories according to the identity of A cations. If A equals noble-metal cation ($A = \text{Cu, Ag}$), the compound adopts chalcopyrite structure (diamond-like or CuFeS_2 type) . If A equals alkali metal ($A = \text{Li, Na}$), the compound crystallizes in orthorhombic $\alpha\text{-NaFeO}_2$ type , a modification of wurtzite type. These three-dimensional networks are both constructed by tetrahedral units via sharing four corners only differ in the stacking sequences of the anions. The chalcopyrite type is a zinc-blende superstructure in which C atoms have an fcc packing, and the orthorhombic type is a wurtzite superstructure in which C atoms are hcp stacked . The cationic noble-metal ($A = \text{Cu, Ag}$) or alkali metal ($A = \text{Li, Na}$) provides electron to the corresponding anionic framework; meanwhile, it may participate in constructing the band structure. Relatively, the alkali metal ($A = \text{Li, Na}$) is merely an electron donator and hardly contributes to the frontier orbitals because of the small ion radius and simple extra nuclear electron configuration.

The studied ternary compounds $\text{Cu} - \text{III} - \text{VI}_2$ (III=Ga, In, and VI=S, Se) are direct-gap semiconductors with tetragonal chalcopyrite (CH) crystal structure. This family of materials is relevant in many fields, including nonlinear optics, optoelectronic, and photovoltaic devices.

Recently, the $CuGaS_2$ alloy system has attracted considerable attention, because this material has direct bandgaps, which is in the range desirable for applications in solid state lighting and high-efficiency tandem solar cells . The copper indium/gallium diselenide $Cu(In, Ga)Se_2$ (CIGS) thin-film solar cells have emerged as a technology that could challenge the current hegemony of silicon solar panels . This is possible thanks to the peculiar optical and structural properties of CIGS, which possess an extraordinary stability under operating conditions.

However, among ternary chalcopyrite semiconductors, $CuGaS_2$ may be the most promising material for photovoltaic applications due to the bandgap energy (E_g) of 2.43 eV, which perfectly matches the solar spectrum for energy conversion and to its large absorption coefficient above E_g . Accurate knowledge of the electronic and optical properties of these materials is very important for many of these applications. In spite of the considerable amount of research devoted to these materials, this knowledge is still incomplete.

During the past years, the physical and chemical properties of $CuGaS_2$, semiconductor has been extensively studied. $CuGaS_2$ is an example of the View the MathML source type of compounds predicted by Abrahams and Bernstein S.C. Abrahams and J.L. Bernstein, J. Chem. Phys. 59 (1973), p. 5415. Full Text via CrossRef — View Record in Scopus — Cited By in Scopus (28). Alonso et al. reported on the complex dielectric tensor components of four chalcopyrite semiconductors ($CuInSe_2$, $CuGaSe_2$, $CuInS_2$, and $CuGaS_2$) in an optical energy range not, vert, similar 1.4-5.2 eV. Levchenko et al. measured optical spectra and energy band structure of single crystalline $CuGaS_2$ and $CuInSe_2$. Vidal et al. presented a first-principles study of the electronic properties of $CuIn(S, Se)_2$ (CIS) using state-of-the art self-consistent GW and hybrid functionals. Merino et al. estimated the bond ionicities, f_i, CuC and f_i, BC of several $CuBC_2$ (B=Al, Ga, In, and C=S, Se, Te) chalcopyrite compounds by means of the Phillips-Van Vechten dielectric theory. Chen et al. performed systematic first-principles calculations for the structural and electronic properties of chalcopyrite semiconductors $AgGaS_2$, $AgGaSe_2$, $CuGaS_2$, $CuGaSe_2$, and their alloys. Prabukanthan and Dhanasekaran have grown single crystals of undoped and 1 and 2 mol% Mn doped $CuGaS_2$ (CGS) by the chemical vapor transport method using iodine as the transporting agent. Levchenko et al. determined the exciton

and band parameters as well as the energy band structure at photon energies higher than the fundamental bandgap by investigating the reflectivity and luminescence spectra of $CuGaSe_2$ single crystals.

2 MATERIAL PROPERTIES OF CHALCOPYRITE

A first fundamental work about the growth and the structural characterization of chalcopyrite compounds was published by Hahn et al. in 1953 . Later work on chalcopyrites was mostly motivated by their potential for non-linear optical applications, visible-light emitters, and photodetectors.

In the beginning of the seventies a first comprehensive review of chalcopyrite compounds was given in the book by Shay and Wernick . Later, Pamplin published several reviews about phase formation rules, thermodynamic phase relations, and experimental results of ternary adamantine compounds, among them the Cu-chalcopyrites . Whereas earlier work was almost entirely about single crystal specimen, more recent experimental investigations have been focused on thin films, due to the high potential of these materials for large area photovoltaic modules .

2.0.1 METHODOLOGY

For our electronic structure calculations, we used the well established TB-LMTO method . Electron corrections are taken into account within the local density approximation (LDA) of DFT . The basic of TB-LMTO method starts from the minimal set of mffin tin orbital of a Koringa-Kohn-Rostoker(KKR) formalism and then linearises it by expanding around a nodal energy point .

2.1 CRYSTAL STRUCTURE OF CHALCOPYRITE

The chalcopyrite structure, named after the mineral chalcopyrite $CuFeS_2$ and also adopted by a number of $I - III - VI_2$ and $II - IV - V_2$ compounds, is a ternary-compound equivalent of the diamond structure, in

which every atom is bonded to four first-neighbours in a tetrahedral structure .

There are 36 known ternary $A^I B^{III} C_2^{VI}$ chalcopyrite semiconductors where A= Cu, Ag, B= Al, Ga, In, Ti and C= S, Se, Te.

The chalcopyrite structure can be obtained by doubling the zinc-blende structure along the z-axis and filling the lattice sites .

The anions remain at their sites and every second (001) plane is occupied by cations as shown in Figure . In consequence, each C anion is coordinated by two A and two B cations and each cation is tetrahedrally coordinated by four anions. The tetrahedron is no longer regular but is distorted along the crystal c-axis such that c/a ratio deviates from the ideal value of 2.0 .

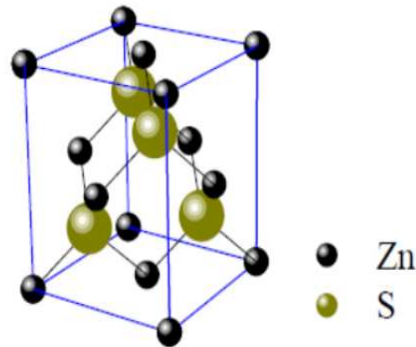
The Bravais lattice of the chalcopyrite is body centered tetragonal.

To describe the crystal structure let us take an example of chalcopyrite . Let us consider the case of $CuInSe_2$

$CuInSe_2$ belongs to the group of ternary chalcopyrite compounds which derives from the group IV class of tetrahedrally bonded semiconductors according to the Grimm-Sommerfeld rule, i.e. there must be an average of 4 valence atoms per atomic site.

In these structures each atom has four neighbors arranged at the corners of a regular tetrahedron bonded by sp^3 bonds. The tetrahedral structure of the chalcopyrites can be considered as a superlattice structure of the sphalerite or zincblende structure which has a diamond like structure (such as Si) consisting of two inter-penetrating face centered cubic lattices, separated by a translation vector of $(\frac{1}{4}\frac{1}{4}\frac{1}{4})$. One sublattice is occupied by cations and the other by anions (II-VI and III-V compounds). In a ternary chalcopyrite the cations are furthermore replaced by a one cation of higher valency and one cation of lower valency which occupy the cation sublattice in an ordered manner as shown in Figure 1. In that sense $CuInSe_2$ can be envisioned as the ternary analogue of the binary ZnS. The reduced symmetry, due to the two kinds of cations, leads to a primitive cell of eight atoms in the chalcopyrite structure compared to a primitive cell of two atoms in the zincblende structure. The Bravais lattice of the chalcopyrite is body centered tetragonal. Compared to the face centered cubic Bravais-cell of the zincblende the unit cell is doubled along the crystal c axis. If the cations are distributed at random, the ternary compound has a sphalerite structure.

2.1.1 ZINC BLEND STRUCTURE



In diamond structure if we substitute Zn and S atoms in place of carbon atoms, then we get zincblende structure .

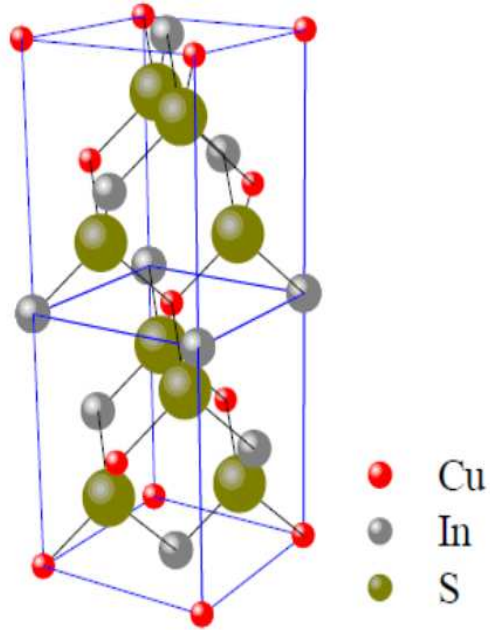
2.1.2 STRUCTURE OF CHALCOPYRITE

As we say above the chalcopyrite structure can be obtained by doubling the zinc-blende structure along the z-axis and filling the lattice sites .

The anions remain at their sites and every second (001) plane is occupied by cations as shown in Figure . In consequence, each C anion is coordinated by two A and two B cations and each cation is tetrahedrally coordinated by four anions. The tetrahedron is no longer regular but is distorted along the crystal c-axis such that c/a ratio deviates from the ideal value of 2.0 .

The Bravais lattice of the chalcopyrite is body centered tetragonal.

Each S atom in the lattice is at the center of a tetrahedron with four cations at each corner. Since in a chalcopyrite structure, in contrast to the zincblende, the sulfur atom is bonded to two types of cations the respective bond lengths are not necessarily identical. As a result the tetrahedron is no longer regular but is distorted along the crystal c-axis such that the c/a ratio



deviates from the ideal value of 2.0 (Figure 3). In addition, the difference in bonding length leads to an internal displacement of the anion away from the ideal position 0.25 a so that the anion sublattice is slightly distorted. In the case of $CuInSe_2$ the Cu-S bond length is 2.335 , whereas the In-S bond length is 2.464 . As a result the sulfur atom moves away from the In-atoms and towards the Cu-atoms resulting in a stretched unit cell with a c/a ratio of 2.014 . In the case of the $CuGaS_2$ lattice the Ga-S bond is shorter than the Cu-S bond, hence the unit cell is compressed with a c/a ratio = 1.97 .

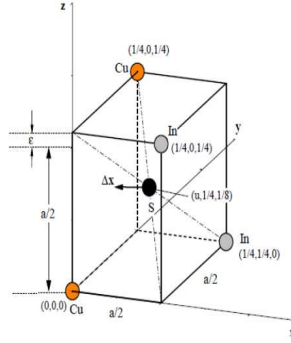


Figure 1.2: Tetrahedron distortion in CuInS_2 . ϵ denotes the tetragonal distortion of the unit cell along the crystal c axis.

3 TYPES OF CHALCOPYRITES

Basically three types of chalcopyrite structures are present .

1. Pure chalcopyrites
2. Defect chalcopyrites
3. Doped chalcopyrites

4 PURE CHALCOPYRITE AND ITS STRUCTURAL AND ELECTRONIC -PROPERTIES

Semiconductors with the formula $I - III - VI_2$ which crystallize in the chalcopyrite structure are the pure chalcopyrites .

received attention recently for their applications in nonlinear optical devices, detectors and solar cells . Among these materials AgGaS_2 and CuGaS_2 have bandgaps in the visible part of the optical spectrum, thus making them more easy to study with visible lasers such as Ar ion and HeCd lasers. In particular, CuGaS_2 has a bandgap of around 2.5 eV and can be doped p-type. Hence it is potentially useful in the fabrication of green light-emitting diodes and lasers in combination with n-type wide bandgap $II - VI$ semiconductors such as CdS . AgGaS_2 , on the other hand, is transparent in the far-infrared for wavelengths from 0.45 to 13 μm . Its linear and nonlinear optical properties

make it a useful material for second harmonic generation and as an optical parametric oscillator. More recently, alloys of these semiconductors have attracted attention as important materials for solar cells . The alloy system $Ag_xCu_{1-x}GaS_2$ is interesting because its band gap exhibits a rather large bowing parameter and can be tuned over a range of 350 meV by varying the amount of Ag. The lattice vibration and bowing parameter of energy band gap in this alloy, which have highly nonlinear optical susceptibility and large birefringence, have been reported . Both $AgGaS_2$ and $CuGaS_2$ compounds represent part of the View the MathML source family type compounds which crystallize in the tetragonal space group View the MathML source with four formula units in each cell, and they have a chalcopyrite structure that is closely related to those of zinc blende and wurtzite structures J.L. Shay and J.H. Wernick, Ternary Chalcopyrite Semiconductors: Growth Electronic Properties and Applications, Pergamon Press, Oxford (1974). These materials are isoelectronic with the zinc blende $II - VI$ compound semiconductors.

4.1 STRUCTURAL PROPERTIES OF PURE CHALCOPYRITE

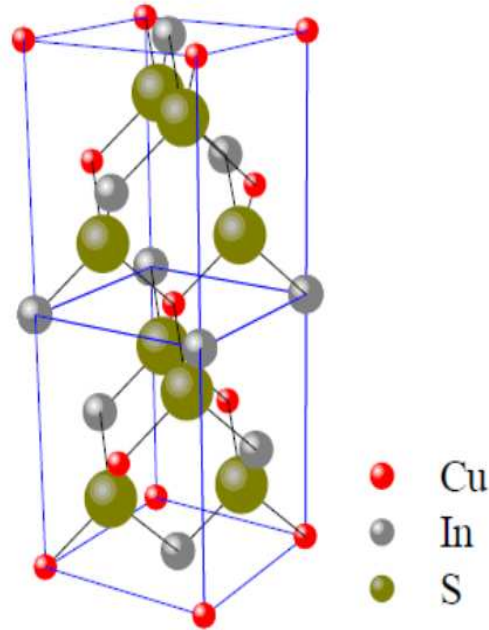
To describe the crystal structure let us take an example of pure chalcopyrite . Let us consider the case of $CuInSe_2$

$CuInSe_2$ belongs to the group of ternary pure chalcopyrite compounds which derives from the group IV class of tetrahedrally bonded semiconductors according to the Grimm-Sommerfeld rule, i.e. there must be an average of 4 valence atoms per atomic site.

In these structures each atom has four neighbors arranged at the corners of a regular tetrahedron bonded by sp^3 bonds. The tetrahedral structure of the chalcopyrites can be considered as a superlattice structure of the sphalerite or zincblende structure which has a diamond like structure (such as Si) consisting of two inter-penetrating face centered cubic lattices, separated by a translation vector of $(\frac{1}{4}\frac{1}{4}\frac{1}{4})$. One sublattice is occupied by cations and the other by anions (II-VI and III-V compounds). In a ternary chalcopyrite the cations are furthermore replaced by a one cation of higher valency and

one cation of lower valency which occupy the cation sublattice in an ordered manner as shown in Figure 1. In that sense $CuInSe_2$ can be envisioned as the ternary analogue of the binary ZnS . The reduced symmetry, due to the two kinds of cations, leads to a primitive cell of eight atoms in the chalcopyrite structure compared to a primitive cell of two atoms in the zincblende structure. The Bravais lattice of the chalcopyrite is body centered tetragonal. Compared to the face centered cubic Bravais-cell of the zincblende the unit cell is doubled along the crystal c axis. If the cations are distributed at random, the ternary compound has a sphalerite structure.

4.1.1 STRUCTURE OF PURE CHALCOPYRITE



These ternary semiconductors crystallize in the chalcopyrite structure which is related to the zinc blende structure. It has nearly the same arrangement of anions but differs in the ordered distribution of the cations which makes the unit cell tetragonal with the c-axis about twice the a-axis of the zinc blende type unit cell, since each anion is coordinated by two A and B cations, while each anion is tetrahedrally coordinated by four anions . The

atomic positions are given as follows: A(0, 0, 0), (0, 1/2, 1/2); B(1/2, 1/2, 0); (1/2, 0, 1/4), C(u, 1/4, 1/8); (u, 3/4, 1/8); (3/4, u, 7/8); (1/4, u, 7/8). In the crystals considered here, the geometrical parameter $\eta = c/2a$ is less than 1, the reason for this distortion is caused by second neighbor interactions. The anions are displaced from their ideal tetrahedral sites by an amount u which is a function of the lattice constants as given by

$$u = \frac{1}{2} - \left[\frac{c^2}{32a^2} - \frac{1}{16} \right]^{\frac{1}{2}} \quad (1)$$

Also, there are two cations sublattices rather than one, leading to the existence of two basic near-neighbor chemical bonds A-C and B-C, with generally unequal bond lengths $R_{AC} \neq R_{BC}$. Thus, the two near-neighbor distances are given by

$$R_{AC} = a \left[u^2 + \frac{(1 + \eta^2)}{16} \right]^{\frac{1}{2}} \quad (2)$$

and

$$R_{BC} = a \left[\left(u^2 - \frac{1}{2} \right)^2 + \frac{(1 + \eta^2)}{16} \right]^{\frac{1}{2}} \quad (3)$$

Hence, the anion displacement $(u - \frac{1}{4}) = \frac{(R_{AC}^2 - R_{BC}^2)}{a^2}$ measures the extent of bond alternations in the system. The structural anomalies(($\eta - 1$) and $(u - 1/4)$) and relative to the ZB structure ($\eta = 1$ and $u = 1/4$) are seen to be significant.

4.2 ELECTRONIC PROPERTIES OF PURE CHALCOPYRITE

4.2.1 METHODOLOGY :

For our electronic structure calculations, we used the well established TB-LMTO method . Electron corrections are taken into account within the local density approximation (LDA) of DFT . The basic of TB-LMTO method starts from the minimal set of mffin tin orbital of a Koringa-Kohn-Rostoker(KKR) formalism and then linearises it by expanding around a nodal energy point .

The ab-initio method is based on Density Functional Theory of Kohn-Sham is used here. The total electronic energy is a function of electron density which is calculated using variational principle. This requires selfconsistent calculations. In practice the Kohn-Sham orbitals are usually expanded in terms of some chosen basis function.

4.2.2 RESULT AND DISCUSSION

Structural Properties

Here we calculate the structural properties i.e, the lattice parameters(a and c) and the anion displacement parameter (u) using the TB-LMTO code by minimising the energy .

Here for $CuInSe_2$ $a=5.49$, $c=11.33$ and $u=0.230$

For the result and discussion of electronic properties we take a samples for which we calculate the structural parameters(a,c,u)
The sample here is $CuInSe_2$.

Band structure

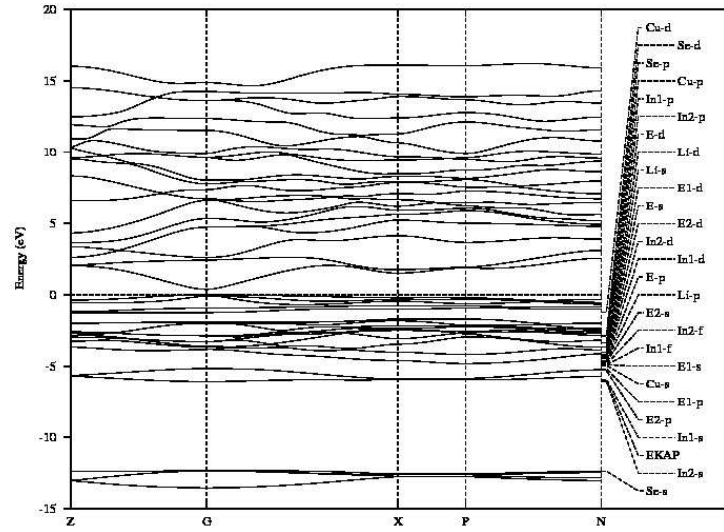
The band structure of $CuInSe_2$ is shown in Figs.5 . The top of the valence bands and the bottom of the conduction bands lie along the Γ -point indicating that compound is direct band gap semiconductor. The bandgaps of theses materials are underestimated in the LDA, when compared with the experimental data . They are smaller than the experimental values and this

is an intrinsic feature of the DFT-LDA. At the center of the Brillouin zone near the VBM, we find the crystal-field pair (singly degenerate) and (doubly degenerate). With the use of the sign convention, the crystal-field (CF) splitting between them is given by $\Delta_{CF} = E(\Gamma'_{5\nu}) - E(\Gamma_{4\nu'})$. It represents the effects of

- (i) existence of two distinct cations (Li) and (Ga,In)
- (ii) tetragonal distortion $\eta \neq 1$, and
- (iii) anion displacement $u \neq 1/4$.

In the zinc-blende structure ($\eta = 1$ and $u = 1/4$) one has $\Delta_{CF} = 0$, and the View the MathML source pair forms the triply degenerate state at VBM. Any of the three factors (i)-(iii) can lead to $\Delta_{CF} \neq 0$. Our calculated value of the crystal-field Δ_{CF} for both compounds are in good agreement with the experiment.

Band structure of $CuInSe_2$:

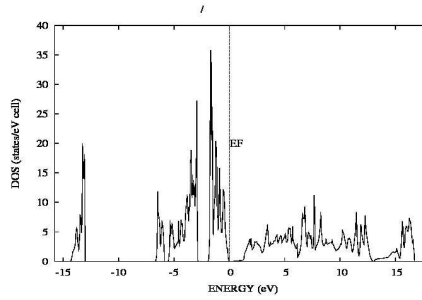


From the above structure it is clear that $CuInSe_2$ have direct band gap, as the minimal state of conduction band and maximal state of valence band are along same line.

Total density of states

we present the calculated total and the angular momentum decomposition of the atom-projected density of states (DOS) of our crystal $CuInSe_2$ in Figs.7 .

Total density of states of $CuInSe_2$:



From the total density of state we calculate the band gap of the chalcopyrite semiconductor which comes :

for $CuInSe_2$ = 1.35

5 DEFFECT CHALCOPYRITE AND ITS STRUCTURAL AND ELECTRONIC -PROPERTIES

The ternary chalcopyrite compounds can be derived from its binary analogs it is possible to further substitute an additional metal M in a ternary $A^I B^{III} X_2^{VI}$ compound without violating the four electrons per lattice site rule. In general in the case of an isovalent substitution, e.g. $A^I B_{1-x}^{III} M_x^{III} X_2^{VI}$ (M substitutes for B), the new quaternary compound will still be a chalcopyrite, whereas a non-isovalent substitution will be accommodated in

the crystal lattice by the formation of associated vacancies, e.g. $A_{1-2x}^I M_x^{II} \square_x B^{III} X_2^{VI}$. These compounds are called defect chalcopyrites.

These can be considered ordered vacancy compounds. For example in a $I - III - VI_2$ compound, we may double the formula unit and then remove one of the group-I elements, thus creating a vacancy and replacing the other group I back by a group-II element to maintain the valency. For example $CuGaSe_2$ can be turned into $Zn\square Ga_2Se_4$, where \square represents the vacancy.

5.1 STRUCTURAL PROPERTIES OF DEFECT CHALCOPYRITE

The chalcopyrite crystal structure has a body-centered tetragonal Bravais lattice for which the primitive unit-cell lattice vectors can be chosen as $(a/2, a/2, 2c/2)$, $(a/2, 2a/2, c/2)$, $(2a/2, a/2, c/2)$. The unit-cell contains two formula units.

The atomic positions are :

I: $(0,0,0), (a/2, 0, c/4)$

III: $(a/2, a/2, 0), (0, a/2, c/4)$

VI: $(ua, a/4, c/8), (-ua, -a/4, c/8), (a/4, -ua, c/8), (-a/4, ua, -c/8)$.

in the ASA LMTO method, we place empty spheres at the positions

E1 : $(0, a/2, 0), (a/2, 0, 0)$

E2 : $(a/4, -a/4, c/8), (-a/4, a/4, c/8), (a/4, a/4, -c/8), (-a/4, -a/4, -c/8)$

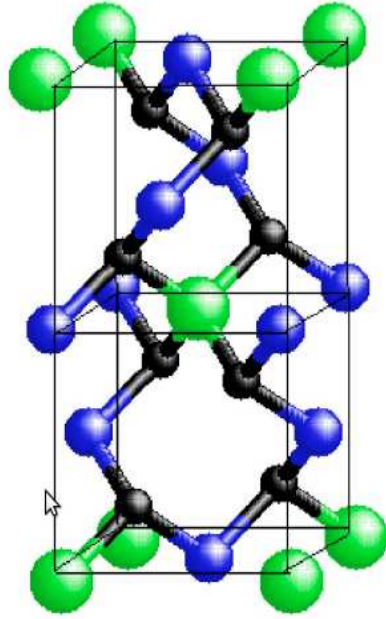
E3 : $(0, 0, c/4), (a/2, a/2, c/4)$.

The ratio $\eta = c/2a$ is 1 for the idealized structure. In most cases, $\eta \leq 1$ and $u \geq 1/4$ which implies that III-VI bond length is shorter than the I-VI bond length.

In the defect chalcopyrite structure, the second of the group-I elements is missing and replaced by an empty sphere of type E4. Furthermore, the posi-

tion of the anion VI now can deviate from the ideal $1/4$ position in all three directions. So, there are now three internal structural parameters (x,y,z) .

5.1.1 CRYSTAL STRUCTURE OF DEFECT CHALCOPYRITE :



(Color online) Defect chalcopyrite crystal structure.

In this crystal structure there are two inequivalent III-VI bond lengths and chemically inequivalent group-III atoms. Thus, the conservation of tetrahedral bond lengths model of Bernard and Zunger³ cannot be used to estimate the internal coordinates.

We adopted the crystal structure of defect chalcopyrite as follows :

II : (0,0,0)
 III: (0,0,1/2), (0,1/2,1/4)
 VI: (x,y,z) , (-x,-y,z) , (y,-x,-z) , (-y,x,-z) .

5.2 ELECTRONIC PROPERTIES OF DEFECT CHALCOPYRITE

5.2.1 METHODOLOGY :

For our electronic structure calculations, we used the well established TB-LMTO method . Electron corrections are taken into account within the local density approximation (LDA) of DFT . The basic of TB-LMTO method starts from the minimal set of mffin tin orbital of a Koringa-Kohn-Rostoker(KKR) formalism and then linearises it by expanding aroun a nodal energy point .

The ab-initio method is based on Density Functional Theory of Kohn-Sham is used here. The total electronic energy is a function of electron density which is calculated using variational principle. This requires selfconsistent calculations. In practice the Kohn-Sham orbitals are usually expanded in terms of some chosen basis function.

5.2.2 RESULT AND DISCUSSION

Structural Properties

Here we calculate the stuctural parameters i.e, the lattice parameters(a and c) and the anion displacement parameter (u_x, u_y and u_z) using the TB-LMTO code by minimising the energy .

Here for $AgAl_2Te_4$ we calculate a, c, u_x , u_y , u_z

For the result and discussion of elwctronic properties we take a samples for which we calculate the structural parameters(a,c,u) which is given in the table of above section.

Here we take the sample $AgAl_2Te_4$.

Band structure

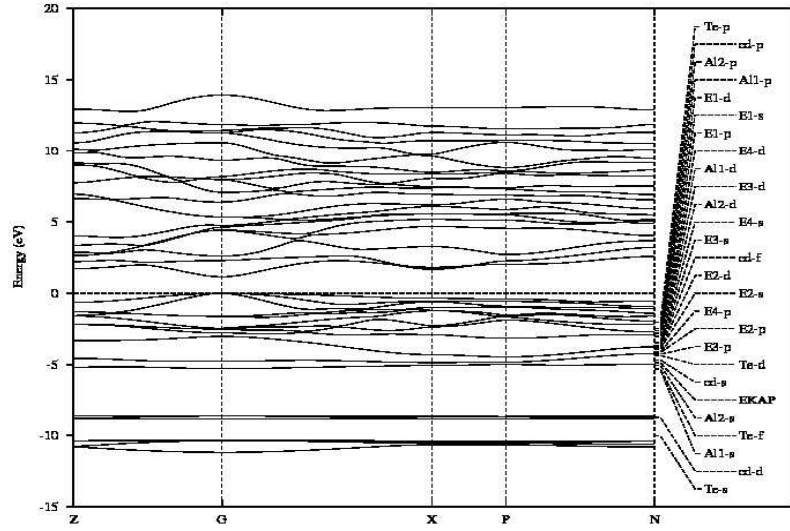
We note that we find all the band gaps of the $II - III_2 - VI_4$ compounds to be direct. In most of these compounds, the nature of the band gap has been under discussion. For instance, in CdGa₂S₄ , an indirect gap of 3.05 eV was reported by Radautsan et al.,²⁷ while a direct gap of 3.44 eV was reported by Kshirsagar and Sinha²⁸ both based on absorption measurements.

Mostly, the suggestions of indirect gaps are based on the observation of weak absorption band tails. Our results strongly suggest that alternative explanations in terms of defects or disorder must be invoked to explain these absorption tails.

Finally, we examine the chemical trends of the band gaps. Clearly, since the gap shifts are not very material dependent, these trends are already clear from the LDA gaps.

Here we show the band structure of defect chalcopyrite $AgAl_2Te_4$.

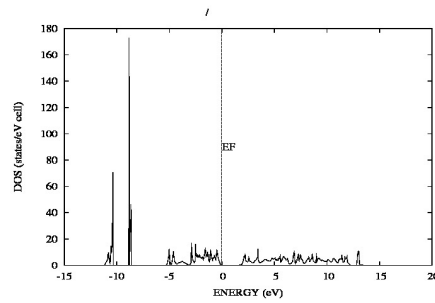
Band structure of $AgAl_2Te_4$:



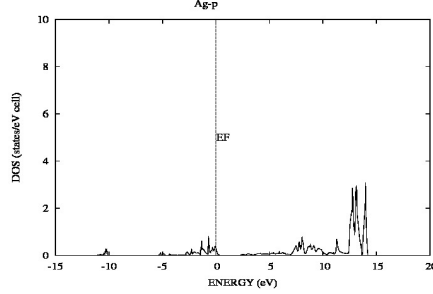
From the above structure it is clear that $AgAl_2Te_4$ have direct band gap, as the minimal state of conduction band and maximal state of valence band are along same line .

Total and partial density of states

Total density of states of $AgAl_2Te_4$:



Partial density of states of $AgAl_2Te_4$: From the total density of state



we calculate the band gap of the chalcopyrite semiconductor which comes :

for $AgAl_2Te_4 = 1.72$

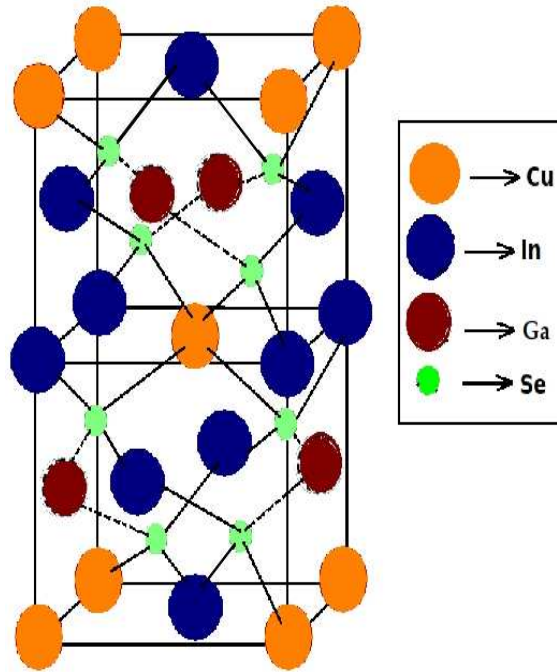
6 DOPED CHALCOPYRITE AND ITS STRUCTURAL AND ELECTRONIC -PROPERTIES

The ternary chalcopyrite compounds can be derived from its binary analogs it is possible to further substitute an additional metal M in a ternary $A^I B^{III} X_2^{VI}$ compound without violating the four electrons per lattice site rule. In general in the case of an isovalent substitution, e.g. $A^I B_{1-x}^{III} M_x^{III} X_2^{VI}$ (M substitutes for B), the new quaternary compound will still be a chalcopyrite, whereas a non-isovalent substitution will be accommodated in the crystal lattice by the formation of associated vacancies, e.g. $A_{1-2x}^I M_x^{II} \square_x B^{III} X_2^{VI}$. These compounds are called defect chalcopyrites. If we dope a atom in the vacant space of defect chalcopyrite then it is called doped chalcopyrite .

6.1 STRUCTURAL PROPERTIES OF DOPED CHA-

LCOPYRITE In case of doped chalcopyrite the crystal structure is same as that of defect chalcopyrite but here in case of doped chalcopyrite we doped a material in the vacancy present in the defect chalcopyrite.

6.1.1 CRYSTAL STRUCTURE OF DOPED CHALCO-PYRITE :



6.2 ELECTRONIC PROPERTIES OF DOPED CHAL-

COPYRITE The electronic structure of these doped chalcopyrites is characterized in almost all cases, except when Cu is substituted by Ge, by a partially full intermediate band (IB) in the gap. Because of the DFT-LSDA gap substitution, the absolute position of this band with respect to the valence band (VB) and to the conduction band (CB) edges is difficult to

determine. For the chalcopyrites, both the VB and the CB edges have a high contribution of the anion orbitals. The IB also has a contribution of the X anion orbitals. The two subgaps between the VB and the IB, and between the IB and the CB will be subestimated similarly because their edges have the same anion character.

6.2.1 METHODOLOGY

For our electronic structure calculations, we used the well established TB-LMTO method . Electron corrections are taken into account within the local density approximation (LDA) of DFT . The basic of TB-LMTO method starts from the minimal set of mffin tin orbital of a Koringa-Kohn-Rostoker(KKR) formalism and then linearises it by expanding around a nodal energy point .

The ab-initio method is based on Density Functional Theory of Kohn-Sham is used here. The total electronic energy is a function of electron density which is calculated using variational principle. This requires selfconsistent calculations. In practice the Kohn-Sham orbitals are usually expanded in terms of some chosen basis function.

6.2.2 RESULT AND DISCUSSION

Structural Properties

Here we calculate the structural parameters i.e, the lattice parameters(a and c) and the anion displacement parameter (u_x, u_y and u_z) using the TB-LMTO code by minimising the energy .

For the result and discussion of electronic properties we take a samples for which we calculate the structural parameters(a,c,u) which is given in the table of above section.

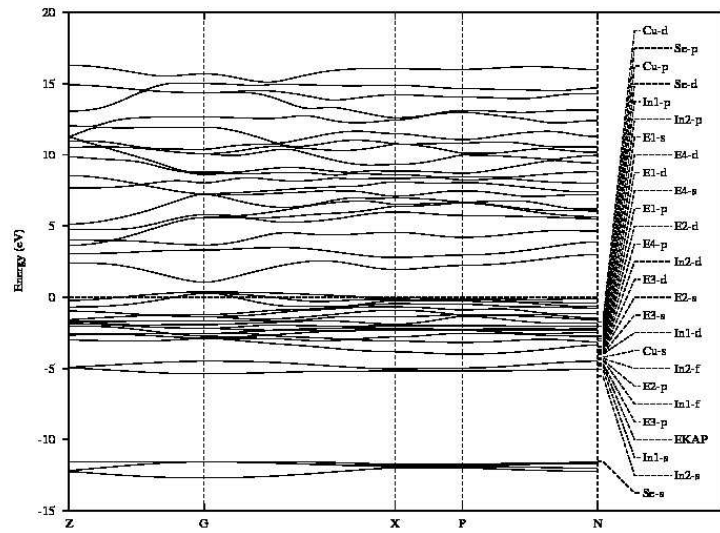
Let the sample is $CuInGaSe_2$.

Band structure

We note that we find all the band gaps of the d compounds to be direct. In most of these compounds, the nature of the band gap has been under discussion. Finally, we examine the chemical trends of the band gaps. Clearly, since the gap shifts are not very material dependent, these trends are already clear from the LDA gaps.

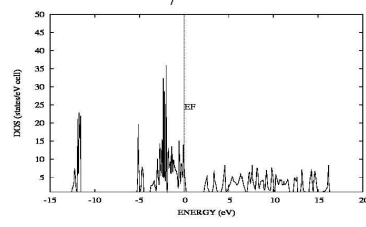
Here we show the band structure of deffect chalcopyrite $CuInGaSe_2$.

Band structure of $CuInGaSe_2$:

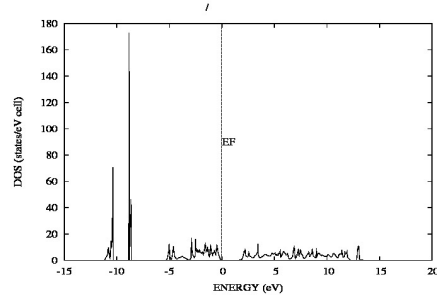


From the above structure it is clear that $CuInGaSe_2$ have direct band gap, as the minimal state of conduction band and maximal state of valence band are along same line .

Total density of states of $CuInGaSe_2$:



Partial density of states of $CuInGaSe_2$:



From the total density of state we calculate the band gap of the chalcopyrite semiconductor which comes : for $CuInGaSe_2 = 1.94$

7 APPLICATION OF CHALCOPYRITE

1. Semiconductors with the formula $I - III - VI_2$ which crystallize in the chalcopyrite structure have received attention recently for their applications in nonlinear optical devices, detectors and solar cells .
2. They have potential optoelectronic applications as solar energy converters, nonlinear optical (NLO) devices, light emitting diodes (LED), and detectors .
3. The chalcopyrite compound $CuInSe_2$ and alloys of the $CuInS_2 - CuGaS_2$ system have been used as absorber layers for thin film solar cells.
4. They reduce nucleation and improve crystal morphology.
5. They are useful for nonlinear optical frequency conversion applications.
6. $Cu - III - VI_2$ (III=Al, Ga and VI=S, Se) chalcopyrite semiconductors¹ are candidates for several optoelectronic applications because of their band gap energies.
7. It has application in photo- voltaic devices .
8. Recently, the $CuGaS_2$ alloy system has attracted considerable attention, because this material has direct band gaps, which is in the range desirable for applications in solid state lighting and high- efficiency tandem solar cells.

8 CONCLUSION

We have studied the structural and electronic properties of pure, defect and doped chalcopyrite semiconductors using Density functional theory (DFT) based first principle technique within Tight binding Linear Muffin Tin orbital (TB-LMTO) method. Our calculated structural parameters such as lattice constant, anion displacement parameter(u) in case of pure chalcopyrite and anion displacement parameter(u_x, u_y, u_z) in case of defect and doped chalcopyrite, tetragonal distortion($\eta=c/2a$) and bond length are in good agreement with other work. Band structure, partial density of states and total density of states of all these chalcopyrites are calculated. The band gaps of these chalcopyrites are in good agreement with experimental results.

9 REFERENCES

1. S.Mishra,B.Ganguli, Solid State Commun.151(2011) 523-528.
2. S.Mishra,B.Ganguli, J.Solid State Chemistry (article in press 2011).
3. W.N.Honeyman, K.H. Wilkinson,J.Phys.D:Appl.Phys.4(1971)1182.
4. B.Tell,J.L.Shay,H.M.Kasper,Phys.Rev.B9(1974)5203.
5. O.Jepsen,O.K.Andersen,Solid State Commun.9(1971)1763.
6. L.L.Kazmerski,Nuovo Cimento D2(1983)2013.
7. J.L.Shay,L.M.Schiavone,E.Buehier,J,H.Wernick,J.Appl.Phys.43(1972)2805.
8. H.Horinaka,S.Mononobe,N.Yamamoto,Japan.J.Appl.Phys32(Suppl.32-33)(1993)109.
9. F.K.Hopkins,Laser Focus World 31(1995)83.
10. A.H.Reshak,S.Auluck,Solid State Commun. 145(2008)571
11. O.K.Andersen,pHYS.Rev.B 12(1975)3060.
12. J.E.Jaffe,A.Zunger,Phys.Rev.B 29(1984)1882.
13. W.Kohn,L.J.Sham,Phys.Rev.A 140(1965)1133.
14. P.Hohenberg,W.Kohn,Phys.Rev.B 136(1964)864.
15. K.Sato.Mater.Sci.Semicond.Process.6(2003)335